J Fluoresc (2015) 25:1681–1693
DOI 10.1007/s10895-015-1655-5

ORIGINAL ARTICLE

Interaction Behavior Between Niclosamide and Pepsin Determined by Spectroscopic and Docking Methods

Liuqi Guo[1] · Xiaoli Ma[1] · Jin Yan[1] · Kailin Xu[1] · Qing Wang[1] · Hui Li[1]

Received: 21 June 2015 / Accepted: 9 September 2015 / Published online: 26 September 2015

Abstract The interaction between niclosamide (NIC) and pepsin was investigated using multispectroscopic and molecular docking methods. Binding constant, number of binding sites, and thermodynamic parameters at different temperatures were measured. Results of fluorescence quenching and synchronous fluorescence spectroscopy in combination with three-dimensional fluorescence spectroscopy showed that changes occurred in the microenvironment of tryptophan residues and the molecular conformation of pepsin. Molecular interaction distance and energy-transfer efficiency between pepsin and NIC were determined based on Förster nonradiative energy-transfer mechanism. Furthermore, the binding of NIC inhibited pepsin activity in vitro. All these results indicated that NIC bound to pepsin mainly through hydrophobic interactions and hydrogen bonds at a single binding site. In conclusion, this study provided substantial molecular-level evidence that NIC could induce changes in pepsin structure and conformation.

Keywords Niclosamide · Pepsin · Binding · Fluorescence spectroscopy · Molecular modeling

Introduction

Niclosamide (NIC; 2′,5-dichloro-4′-nitrosalicylanilide; Fig. 1) is an anthelmintic drug that is extensively used to treat various worm infestations [1]. NIC has also been used for antibacterial and antitumor therapies [2–4]. NIC represents a potential drug candidate for the effective treatment of severe acute respiratory syndrome (SARS) coronavirus infection against SARS [5].

Pepsin, the main digestive enzyme, is crucial for digestive processes in the stomach. Pepsin is synthesized from pepsinogen and secreted by gastric chief cells [6, 7]. Pepsin has a single polypeptide enzymatic chain containing 324 amino acid residues and a molecular mass of 35 000 Da [8]. Pepsin is a member of the large family of aspartic proteases, which are of significant medical and pharmaceutical interest because several of these enzymes have important roles in the development of various human diseases, formation of gastric ulcers, HIV maturation, and use as prognostic tools for breast-tumor invasiveness [9]. The drug interacts with pepsin when upon entering the stomach [10]. Several reports on the interactions of several molecules with pepsin have been published [11–15]. Recently, Esra Maltas [16] reported the interactions of NIC with several proteins, including human serum albumin, hemoglobin, and globulin. However, to the best of our knowledge, only a few studies focused on the interaction behavior between NIC and pepsin. The interaction of NIC with pepsin and enzymes can provide useful information on drug action and explain its mechanism of action in the human body.

In the present study, the interaction behavior between NIC and pepsin was investigated using fluorescence spectroscopy, synchronous fluorescence spectroscopy, three-dimensional fluorescence spectra, and molecular modeling. The quenching mechanism, measured binding constants, binding sites, and molecular interaction distance were investigated. The binding model between NIC and pepsin was established. The study would facilitate further investigation of the interaction mechanisms of NIC with pepsin and lead to the identification of new targets for pepsin-related disorder.

✉ Hui Li
lihuilab@sina.com

[1] College of Chemical Engineering, Sichuan University, Chengdu, Sichuan 610065, People's Republic of China

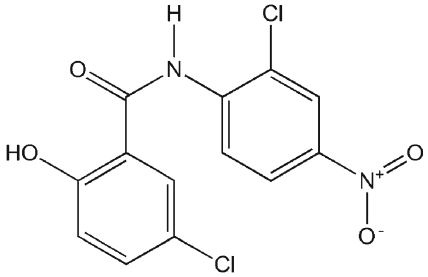

Fig. 1 Molecular structure of NIC

Experimental

Reagents

Porcine pepsin was purchased from Sigma-Aldrich Chemical Co. (St. Louis, MO, USA) and NIC was obtained from the AiKeDa Chemical Co., Ltd. (Chengdu, China). Pepsin stock solution was prepared at a concentration of 1.0×10^{-3} mol·L^{-1} in citric acid–sodium citrate buffer solution of pH 2.0 (0.2 mol·L^{-1}, containing 0.1 mol·L^{-1} NaCl). A solution of NIC (2.0×10^{-3} mol·L^{-1}) was first prepared in anhydrous methanol. All chemicals were of analytical grade and used without further purification. Water was purified using the Millipore purification system (Barnstead, NH, USA). All stock solutions were stored at 0 to 4 °C.

Equipment and Spectral Measurements

The fluorescence spectra were obtained using the Cary Eclipse fluorescence spectrophotometer (Varian, Palo Alto, CA, USA) equipped with 1.0 cm quartz cells. The excitation wavelength was 280 nm for all cases, with excitation and emission slits of 5 and 10 nm, respectively. UV–vis spectrum scanning was conducted using the TU-1901 UV–vis spectrophotometer (Persee, Beijing, China).

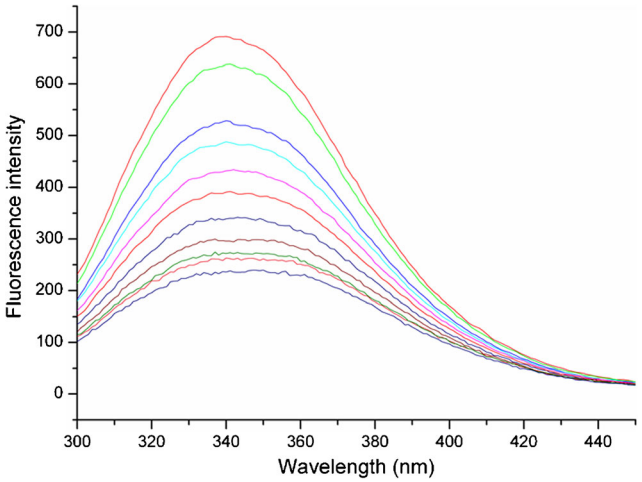

Fig. 3 Fluorescence emission spectra of pepsin in the presence of increasing NIC concentration. Peaks from top to bottom denote C_{NIC} = (0, 5.0, 10.0, 15.0, 20.0, 25.0, 30.0, 35.0, 40.0, 45.0, 50.0)$\times10^{-6}$ mol·L^{-1}, $C_{pepsin}=1.0\times10^{-4}$ mol·L^{-1}

Procedures

A stabilized pepsin concentration (1.0×10^{-4} mol·L^{-1}) with different NIC concentrations (varying from 0 to 50.0×10^{-6} mol·L^{-1}) was added to each 5-mL volumetric flask. The total volume was fixed at 5 mL with citric acid–sodium citrate buffer (pH 2.0). All solutions were mixed thoroughly and held in a thermostat water bath for 30 min before the fluorescence spectra were obtained at different temperatures (293, 301, and 310 K). The synchronous fluorescence spectra of pepsin in the presence of NIC were recorded at 293 K, and the D value ($\Delta\lambda$) between excitation and emission wavelengths was stabilized at 15 or 60 nm, respectively. Three-dimensional fluorescence spectra were obtained under the following conditions: the emission wavelength range was selected from 250 to 500 nm, the initial excitation wavelength

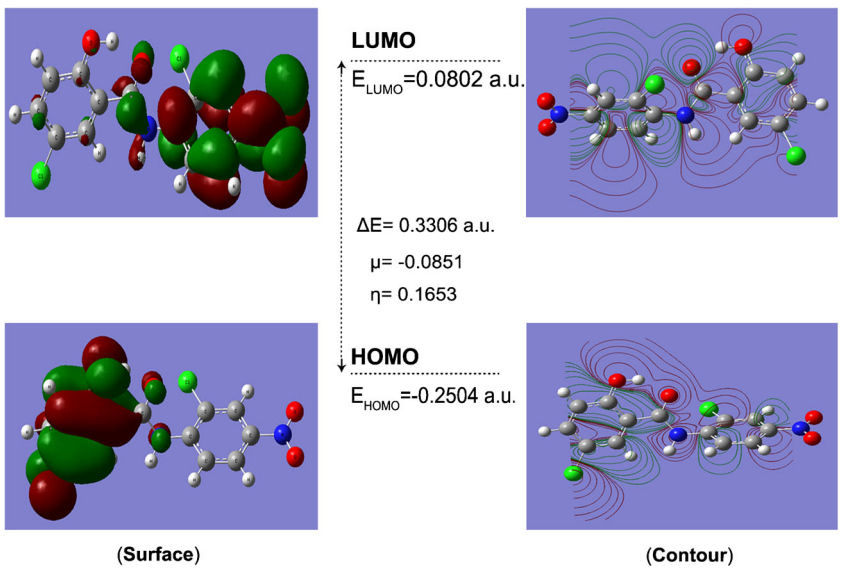

Fig. 2 Surfaces and contours of the molecular orbital plots (HOMO and LUMO) of NIC

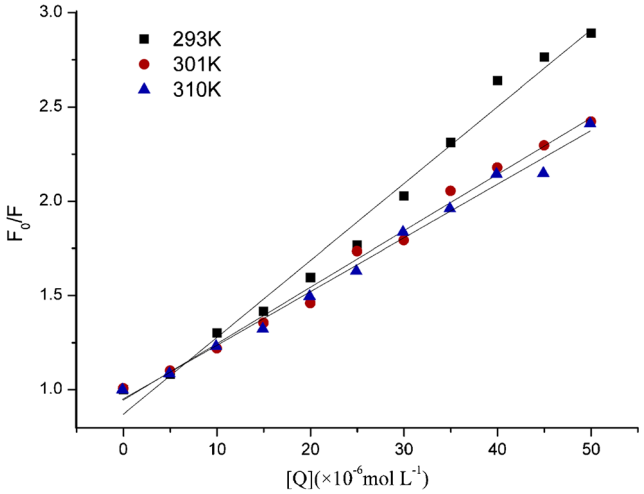

Fig. 4 Stern–Volmer plots for the quenching of pepsin by NIC at different temperatures (293, 301, and 310 K)

was set to 200 nm, and the scanning number was 15 with the increment of 10 nm. The UV–vis absorbance spectra of the NIC–pepsin system were recorded at 293 K.

Molecular Docking Investigation

The molecular docking of NIC with pepsin was investigated using AutoDock 4.2.6 to determine the preferred binding sites of NIC on pepsin and the additional information on the binding structure of NIC and pepsin. The crystal structure of pepsin was obtained from the Brookhaven Protein Data Bank (ID: 5PEP). All water molecules were removed, and Gasteiger charges were added at the beginning of docking study. The geometry of NIC was optimized using density functional theory (DFT) B3LYP/6-311^{+2}G(d,p) by Gaussian 09 (Revision A.01) until all eigenvalues of the Hessian matrix were positive. Using AutoDock 4.2.6, the ligand root of NIC was detected and rotatable bonds were defined. Docking was conducted with grid box size setting of 90 Å×100 Å×90 Å along the *x*-, *y*-, and *z*-axes, respectively, covering the entire protein with Kollman charges to detect the binding sites in pepsin. The grid center was set to −17.802, 40.376, and 86.848 Å for the *x*-, *y*-, and *z*-axes, respectively. Docking simulations were conducted with 200 runs, 2,500,000 energy evaluations, and 25,000 generations. Other parameters used were default values. Finally, the lowest energy conformation was used for docking analysis.

Pepsin Activity Measurement

Anson's [17] method, with some modifications, was used to detect pepsin activity. Pepsin (1.0×10^{-5} mol·L^{-1}) in citric acid–sodium citrate buffer was mixed with different NIC concentrations (0, 1.0, 2.0, 3.0, 4.0, 5.0, 6.0, 7.0, 8.0, 9.0, and 10.0×10^{-5} mol·L^{-1}) at 310 K for 20 min. Then, 2 mL of bovine hemoglobin (0.5 wt.%) solution was added to the aforementioned solutions. After 20 min, 2 mL of 10 wt.% trichloroacetic acid was added to terminate the reaction. The mixture was incubated for 10 min and centrifuged at 12 000 rpm for 20 min. Finally, the OD_{275} value was obtained using a spectrophotometer. Each experiment was repeated three times to determine the mean. The original activity of pepsin was 3000 NFU/mg, and the activity of pepsin in the presence of NIC can be calculated using Eq. (1), written as follows:

$$Activity\left(\frac{\mathrm{NFU}}{\mathrm{mg}}\right) = 3000 \times \frac{OD_{275}(\mathrm{NIC-pepsin})}{OD_{275}(\mathrm{pepsin})} \quad (1)$$

Results and Discussion

Molecular Properties of NIC

The quantitative structure-activity relationship can be applied to predict biological activity based on chemical structures or properties [18].

Based on conceptual DFT [19], chemical potential (μ) and chemical hardness (η) are defined as follows:

$$\chi = -\mu = -\left(\frac{\partial y}{\partial x}\right) v\left(\vec{r}\right) \quad (2)$$

$$\eta = \frac{1}{2}\left(\frac{\partial^2 E}{\partial N^2}\right) v\left(\vec{r}\right) \quad (3)$$

where E is the total energy of the system, N is the number of electrons in the system, is the external potential, and μ is the

Table 1 Stern-Volmer constants for the interaction of pepsin with NIC at different temperatures

T (K)	Equations	$K_{SV}\times10^{-4}$ (L mol^{-1})	$K_q\times10^{-12}$ (L mol^{-1})	R^a
293	$F_0/F=0.408\times10^5$ [Q]+0.8712	4.08	4.08	0.9844
301	$F_0/F=0.299\times10^5$ [Q]+0.9375	2.99	2.99	0.9908
310	$F_0/F=0.285\times10^5$ [Q]+0.9489	2.85	2.85	0.9913

[a] The correlation coefficient

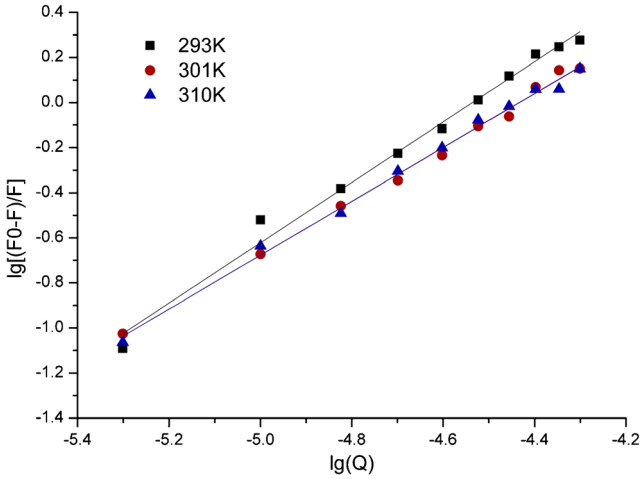

Fig. 5 Double-log plots of the NIC quenching effect on pepsin fluorescence at different temperatures

negative counterpart of electronegativity (χ) as defined by Iczkowski and Margrave [20]. The chemical potential and chemical hardness were calculated using Koopmans' theorem to simply the calculation [21], written as follows:

$$\chi = \frac{E_{\mathrm{LUMO}} + E_{\mathrm{HOMO}}}{2} \tag{4}$$

$$\eta = \frac{E_{\mathrm{LUMO}} - E_{\mathrm{HOMO}}}{2} \tag{5}$$

where E_{LUMO} is the energy of the lowest unoccupied molecular orbital, and E_{HOMO} is the energy of the highest occupied molecular orbital. The surfaces and contours of the HOMO and LUMO plots of the optimized structures of NIC are shown in Fig. 2. Finally, E_{LUMO}, E_{HOMO}, ΔE, μ, η, and the molecular volume of NIC are 0.0802 a.u., −0.2504 a.u., 0.3306 a.u., −0.0851, 0.1653, and 168.173 $\mathrm{cm^3 \cdot mol^{-1}}$, respectively. Notably, charge density was mainly accumulated on the benzene ring and carbonyl group in the HOMO and LUMO. In addition, a significantly large disparity in the distribution of electric charge between HOMO and LUMO was observed. When NIC binds to the amino acid residues of pepsin by charge transfer, the benzene ring and carbonyl group are the main binding groups. Moreover, the binding forces may presumably be π–π stacking or hydrogen bonding. In light of the weak interaction of NIC with pepsin, the ester groups could be the main contributors to the hydrophobic binding force [15]. The results of quantum chemistry calculations can provide a theoretical basis of how to analyze the model of drug binding with pepsin.

Fluorescence Measurement

Fluorescence spectroscopy has been extensively used to investigate the interactions between ligands and proteins and can provide information on the quenching mechanism, binding constants, and binding sites [22–25]. The changes in emission spectra can provide information on a molecule's structure and dynamics [26]. The fluorescence of pepsin is mainly due to tryptophan (Trp) and tyrosine (Tyr) residues. The maximum fluorescence intensities of the Trp and Tyr residues of proteins excited at 280 nm are approximately 340 and 300 nm, respectively [27]. The fluorescence spectra of pepsin at various NIC concentrations are shown in Fig. 3. The fluorescence intensity of pepsin decreased regularly with the increase in NIC concentration, which indicated that NIC was bound to pepsin and affected the structure [10]. Moreover, NIC should be located at or near the Trp residues when it binds with pepsin.

Fluorescence Quenching Mechanism

Fluorescence quenching is the decrease in the quantum yield of fluorescence from a fluorophore induced by a variety of molecular interactions, such as excited-state reactions, energy transfer, ground-state complex formation, and collisional quenching [23]. The different mechanisms of quenching are usually classified as either dynamic quenching or static quenching, which can be distinguished based on different dependencies on temperature and viscosity or preferably by lifetime measurements. Given that a higher temperature resulted in higher diffusion coefficients, the dynamic quenching constants will increase with increasing temperature. By contrast, the increase in temperature is likely to result in decreased stability of complexes. Thus, the values of the static quenching constants are expected to be smaller [22, 28]. The well-known Stern–Volmer equation was used to confirm the mechanism [29], as follows:

$$\frac{F_0}{F} = 1 + K_q \tau_0 [Q] = 1 + K_{SV}[Q] \tag{6}$$

where F_0 and F represent the fluorescence intensity in the absence and presence of the quencher, respectively; $[Q]$ is the concentration of the quencher; τ_0 is the fluorescence lifetime

Table 2 The binding constant K_b and relative thermodynamic parameters of the NIC–pepsin system

T (K)	K_b (L mol^{-1})	n	R^a	ΔH (kJ mol^{-1})	ΔG (kJ mol^{-1})	ΔS (J mol^{-1} K^{-1})
293	1.1809×10^5	1.3388	0.9891	1.665	−34.060	106.86
301	1.9634×10^5	1.1941	0.9957		−30.500	
310	2.0017×10^5	1.1956	0.9952		−31.461	

[a] The correlation coefficient

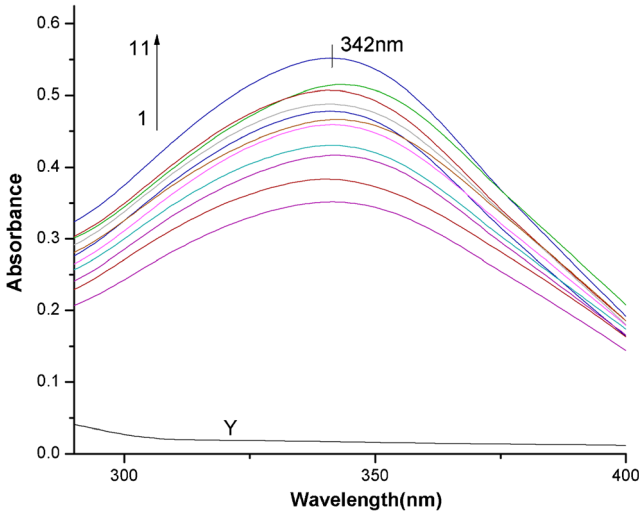

Fig. 6 The UV–vis absorption spectra of 5.0×10^{-5} mol·L^{-1} NIC in the presence of 0.0, 5.0, 10.0, 15.0, 20.0, 25.0, 30.0, 35.0, 40.0, 45.0, and 50.0×10^{-6} mol·L^{-1} pepsin for curves 1–11, respectively. Curve Y shows the absorption spectrum of 50.0×10^{-6} mol·L^{-1} pepsin only

in the absence of the quencher and its value always is 10^{-8} s [30]; K_q is the quenching rate constant of the biological macromolecule; and K_{SV} is the Stern–Volmer quenching constant. In this study, the fluorescence quenching spectra of pepsin in the presence of different NIC concentrations were obtained at three different temperatures (293, 301, and 310 K) to elucidate the quenching mechanism. Figure 4 shows the Stern–Volmer plots for pepsin fluorescence quenching by NIC. The calculated K_{SV} and K_q values are summarized in Table 1. Results show that the K_q value was greater than 2.0×10^{10} L·mol^{-1}·s^{-1}, whereas the maximum diffusion collision quenching rate constant of various quenchers with biopolymer is 2.0×10^{10} L·mol^{-1}·s^{-1} [31]. The above finding indicates a complex formation between protein and quencher, which corresponds to the static mechanism rather than the dynamic collision quenching.

Binding Parameters

For the static quenching process, when small molecules bind independently to a set of equivalent sites on a macromolecule, the binding constant (K_b) and the number of binding sites (n) can be determined by using the following equation [23]:

$$\log\left(\frac{F_0-F}{F}\right) = \log\ K_b + n\log[Q] \tag{7}$$

where $[Q]$ is the concentration of the quencher; F_0 and F are the fluorescence intensity in the absence and presence of the quencher, respectively; K_b is the binding constant; and n is the number of binding sites per pepsin molecule. By plotting $\log(F_0 - F)/F$ versus $\log[Q]$ (as shown in Fig. 5), n and $K_b$can be calculated. The results are summarized in Table 2. Notably, the values of n at the experimental temperatures were approximately equal to 1, indicating that the existence of only a single binding site in pepsin for NIC. The value of K_b is 1.1809×10^5 L·mol^{-1} at room temperature, indicating that a strong interaction exists between NIC and pepsin. To improve the credibility of the combination results, absorption–titration experiments were conducted. The UV–vis spectra of NIC with various pepsin concentrations at 293 K are given in Fig. 6. NIC showed maximum absorption at 343 nm, while pepsin showed no absorption from 290 to 400 nm. As the pepsin concentration increased, the absorption of the NIC significantly increased, indicating the formation of the NIC–pepsin complex. The

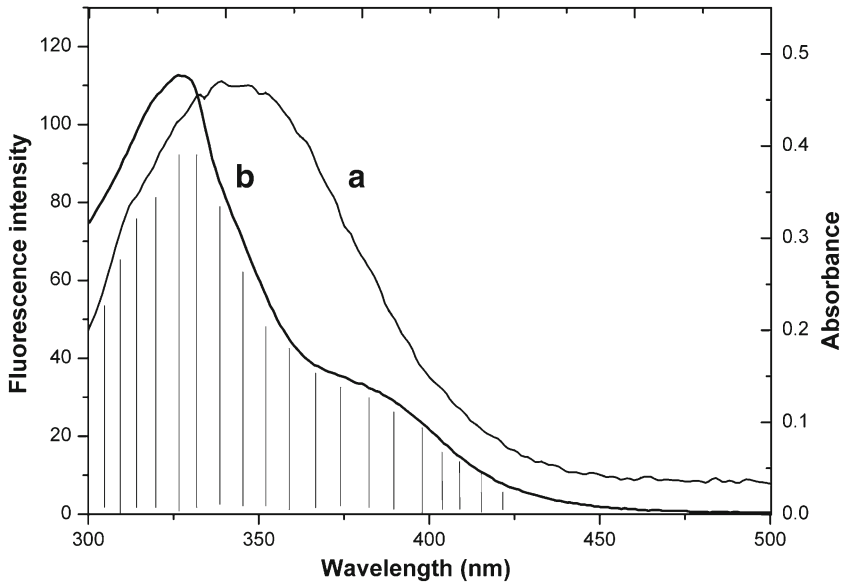

Fig. 7 Overlap of the fluorescence emission of NIC–pepsin (**a**) with the absorption spectrum of NIC (**b**). C_{NIC}= $C_{pepsin}=2.0\times10^{-5}$ mol·L^{-1}

intrinsic binding constant (K_b) can be evaluated using the following equation [32]:

$$\frac{C}{\varepsilon_{a-\varepsilon_f}} = \frac{C}{\varepsilon_{b-\varepsilon_f}} + \frac{1}{K_b\left(\varepsilon_{a-\varepsilon_f}\right)} \tag{8}$$

where C is the concentration of the pepsin, ε_a is the apparent extinction coefficient obtained by calculating the ratio of observed absorbance of NIC–pepsin complex to the NIC concentration ($A_{obs}/[Q]$), ε_f corresponds to the extinction coefficient of the NIC in its free form, and ε_b refers to the extinction coefficient of drug in bound form. K_b can be obtained from the ratio of the slope to the intercept in the plots of $C/(\varepsilon_a - \varepsilon_f)$ versus C. Based on the absorption spectra, the binding constant K_b for NIC and pepsin was 1.83×10^5 L·mol^{-1} at room temperature, which is consistent with the fluorescence quenching data. Thus, NIC can be stored and carried by pepsin. Furthermore, the existence of an independent class of binding sites on pepsin for NIC was inferred based on the values of n.

The Pattern of Interaction Force

Generally, four representative interaction forces, namely, hydrophobic force, hydrogen bond interactions, van der Waals force, and electrostatic interactions, exist between small molecular substrates and biological macromolecules [33]. The aim of this subsection is to attempt to account for the symbols and magnitudes of the thermodynamic parameters of protein association reactions to analyze the molecular forces. The thermodynamic parameters are vital for confirming the intermolecular forces. Ross and Subramanian [34] have summed up the thermodynamic laws to determine the types of binding with various interactions. If $\Delta H < 0$ and $\Delta S < 0$, then van der Waals force and hydrogen bond interactions play the main roles in the binding reaction. If $\Delta H > 0$ and $\Delta S > 0$, then hydrophobic interactions are dominant. If $\Delta H < 0$ and $\Delta S > 0$, then electrostatic interactions are the main driving forces. When the temperature range is narrow, enthalpy change (ΔH) can be regarded as a constant. Enthalpy change (ΔH) and entropy change (ΔS) can help confirm the binding modes. (ΔH) and (ΔS) can be calculated using the Van't Hoff equation, written as follows [35]:

$$\ln K = -\frac{\Delta H}{RT} + \frac{\Delta S}{R} \tag{9}$$

$$\Delta G = -RT\ln K = \Delta H - T\Delta S \tag{10}$$

where K is the binding constant at the corresponding temperature, R is the gas constant, and T is the absolute temperature. The results are presented in Table 2. A negative ΔG indicates that the binding process was spontaneous and enthalpy-driven at the corresponding temperature. The positive ΔH and ΔS values indicate that hydrophobic interactions have major roles

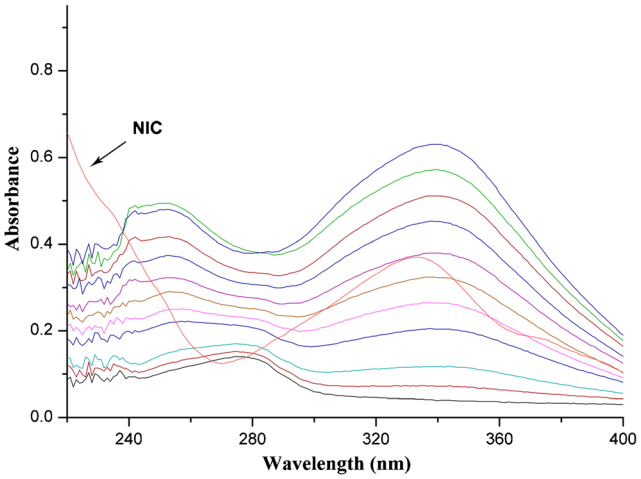

Fig. 8 UV–vis spectra of NIC (2.0×10^{-5} mol·L^{-1}) and pepsin in the presence of different NIC concentrations. Peaks from top to bottom denote C_{NIC}=(50.0, 45.0, 40.0, 35.0, 30.0, 25.0, 20.0, 15.0, 10.0, 5.0, 0)$\times10^{-6}$ mol·L^{-1}, $C_{pepsin}=1.0\times10^{-4}$ mol·L^{-1}

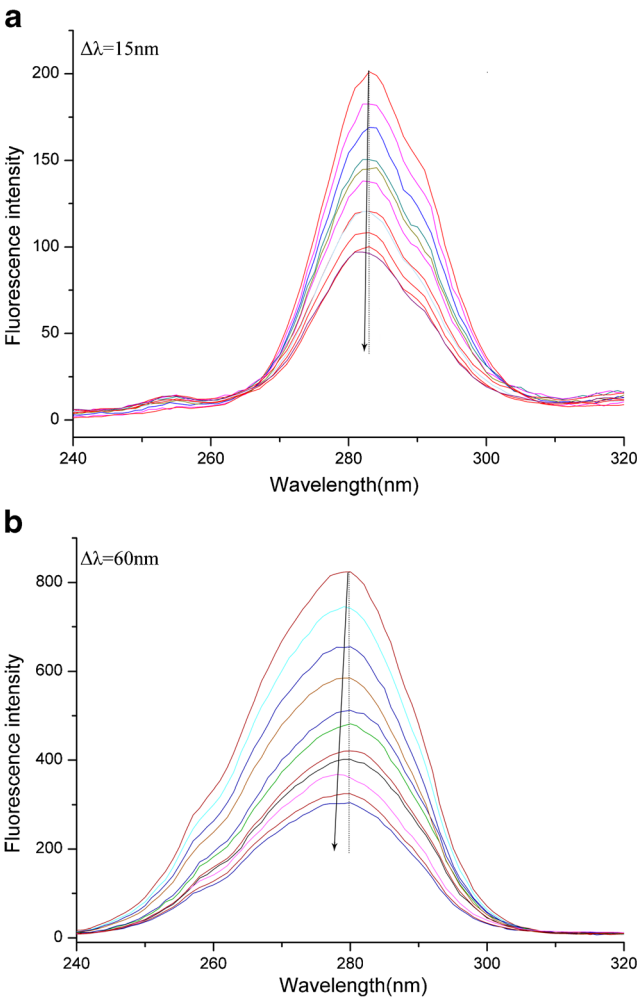

Fig. 9 Synchronous fluorescence spectra of the interaction between pepsin and NIC at (**a**) $\Delta\lambda$=15 nm and (**b**) $\Delta\lambda$=60 nm at room temperature. Peaks from top to bottom denote C_{NIC} = (0, 5.0, 10.0, 15.0, 20.0, 25.0, 30.0, 35.0, 40.0, 45.0, 50.0)$\times10^{-6}$ mol·L^{-1}, $C_{pepsin}=1.0\times10^{-4}$ mol·L^{-1}

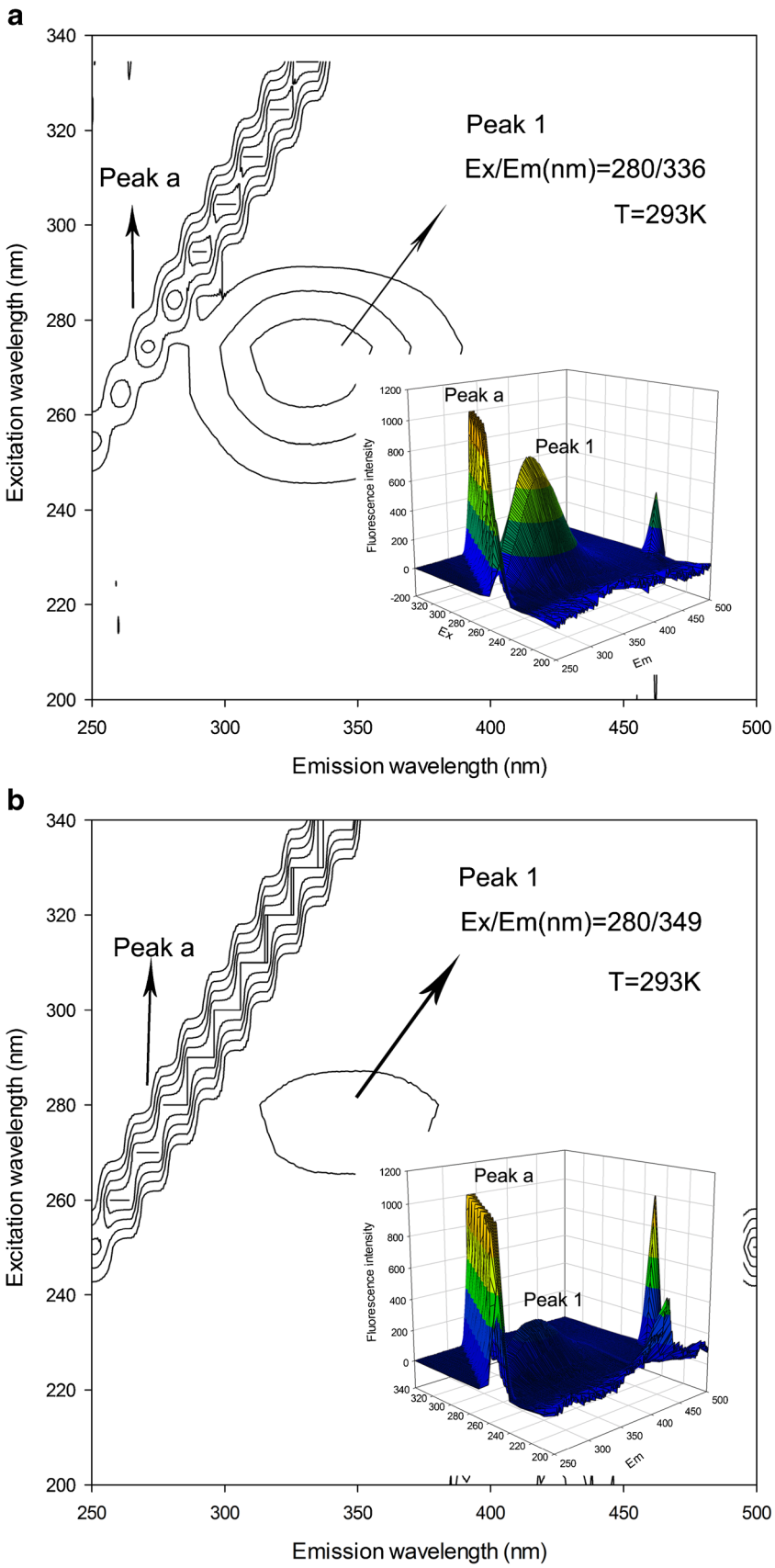

Fig. 10 The three-dimensional fluorescence spectra and contour spectra of pepsin (**a**) and NIC–pepsin system (**b**). a $C_{pepsin}=1.0\times10^{-4}$ mol·L^{-1}, $C_{NIC}=0.0$ mol·L^{-1}; b $C_{pepsin}=1.0\times10^{-4}$ mol·L^{-1}, $C_{NIC}=50.0\times10^{-6}$ mol·L^{-1}

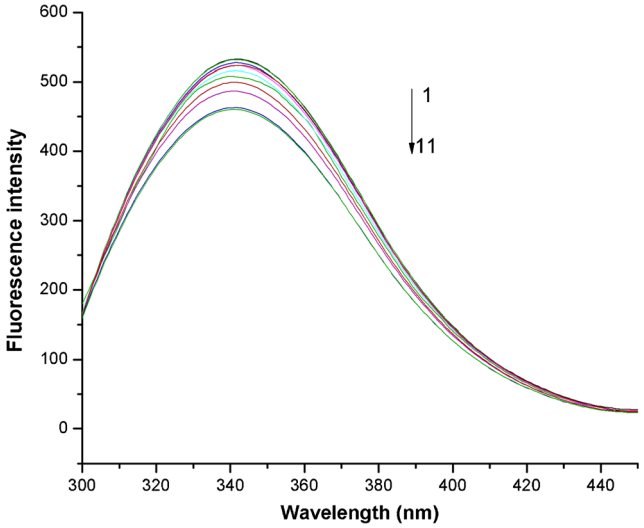

Fig. 11 Effect of NaCl concentration on the fluorescence of NIC–pepsin. C_{NaCl} are 0.1, 0.2, 0.3, 0.4, 0.5, 0.75, 1.0, 1.25, 1.5, 1.75, and 2.0 mol mol·$L^{-1}L^{-1}$ for curves 1 to 11 respectively; $C_{pepsin}=1.0\times10^{-4}$ mol mol·$L^{-1}L^{-1}$; $C_{NIC}=1.0\times10^{-5}$mol mol·$L^{-1}L^{-1}$

in the binding between NIC and pepsin. Results from the present study and other reports showed that binding of many small molecules pepsin occurred via a static quenching mechanism [7, 10, 11, 36–38]. Notably, Li Zhen et al. studied the binding between pepsin and nucleoside analogs (FNC, CYD, and CMP) via a static quenching mechanism. In addition, the effects of molecular structure on the binding aspects have also been compared [12]. Curcumin [7] binding with pepsin mainly through hydrophobic interactions with one binding site, while pepsin bind with silybin [10], and nobilietin [37] mainly through hydrophobic and electrostatic interactions. Chlorogenic acid [38] and pepsin were mainly strengthened by Van der Waals' forces and hydrogen bonds. Furthermore, the binding affinity or binding constants varied. The binding constants for NIC and pepsin calculated using fluorescence data and UV–vis absorption spectra were at the order of magnitude of 10^5 L·mol^{-1} and similar to the nobiletin-pepsin system [37]. The binding constant for fleroxaci [13] and ligupurpuroside A [36] were 10^6 L·mol^{-1}, and prulifloxacin [39] has the binding constant of 10^8 L·mol^{-1}. Results showed that prulifloxacin binds at higher affinity to pepsin than other drugs.

Energy Transfer from Pepsin to NIC

Based on Förster theory of nonradiative energy transfer [40], energy transfer occurs under the following conditions: (a) the donor can produce fluorescence that has a sufficiently long lifetime; (b) the fluorescence emission spectrum of the donor and the UV–vis absorption spectrum of the acceptor overlap; and (c) the distance between donor and acceptor is less than 8 nm. The efficiency (E) of energy transfer between donor and acceptor could be calculated using the following equation [41]:

$$E = 1-\frac{F}{F_0} = \frac{R_0^6}{R_0^6 + r^6} \tag{11}$$

$$R_0^6 = 8.8 \times 10^{-25} k^2 n^{-4} \Phi J \tag{12}$$

where r represents the distance between donor and acceptor, R_0 is the critical distance at which transfer efficiency equals to 50 %, k^2 is the orientation factor related to the geometry of the donor–acceptor dipole, n is the refractive index of the medium, Φ is the fluorescence quantum yield of the donor, and J is the degree of spectral overlap between donor emission and acceptor absorption, which could be calculated by using the following equation:

$$J = \frac{\int_0^\infty F(\lambda)\varepsilon(\lambda)\lambda^4 d\lambda}{\int_0^\infty F(\lambda)d\lambda} \tag{13}$$

where $F(\lambda)$ is the fluorescence intensity of the donor at the wavelength range and $\varepsilon(\lambda)$ is the molar absorption coefficient of the acceptor at the wavelength range. The overlap of the absorption spectrum of NIC and the fluorescence emission spectrum of pepsin is shown in Fig. 7. The overlap integral J can be evaluated by integrating the spectra in Fig. 6 based on Eq. (13). In the present case, $k^2=2/3$, $n=1.36$, and $\Phi=0.15$ [42]. Based on Eqs. (11) to (13), the values of the parameters were determined to be $J=4.761\times10^{-15}$ cm^3·L·mol^{-1}, $R_0=2.23$ nm, $E=0.35$, and $r=2.47$ nm. The maximal academic critical distance for R_0 ranges from 5 to 10 nm, and the maximum academic distance between donor and acceptor for r_0

Table 3 The lowest energy ranked results of five NIC–pepsin binding conformations

Energy ranked results	Conformation data				
	1	2	3	4	5
Binding energy (kcal mol^{-1})	−4.28	−4.12	−3.97	−3.86	−3.67
Ligand efficiency (kcal mol^{-1})	−0.2	−0.2	−0.19	−0.18	−0.17
Inhibition constant (μM)	726.55	954.07	1.23	1.48	2.03
Intermolecular energy (kcal mol^{-1})	−5.48	−5.31	−5.16	−5.05	−4.87

ranges from 7 to 10 nm [27]. The donor to acceptor distance was less than 8 nm, indicating the high possibility of energy transfer from NIC to pepsin occurred. The above result was in accordance with the conditions of Förster theory of

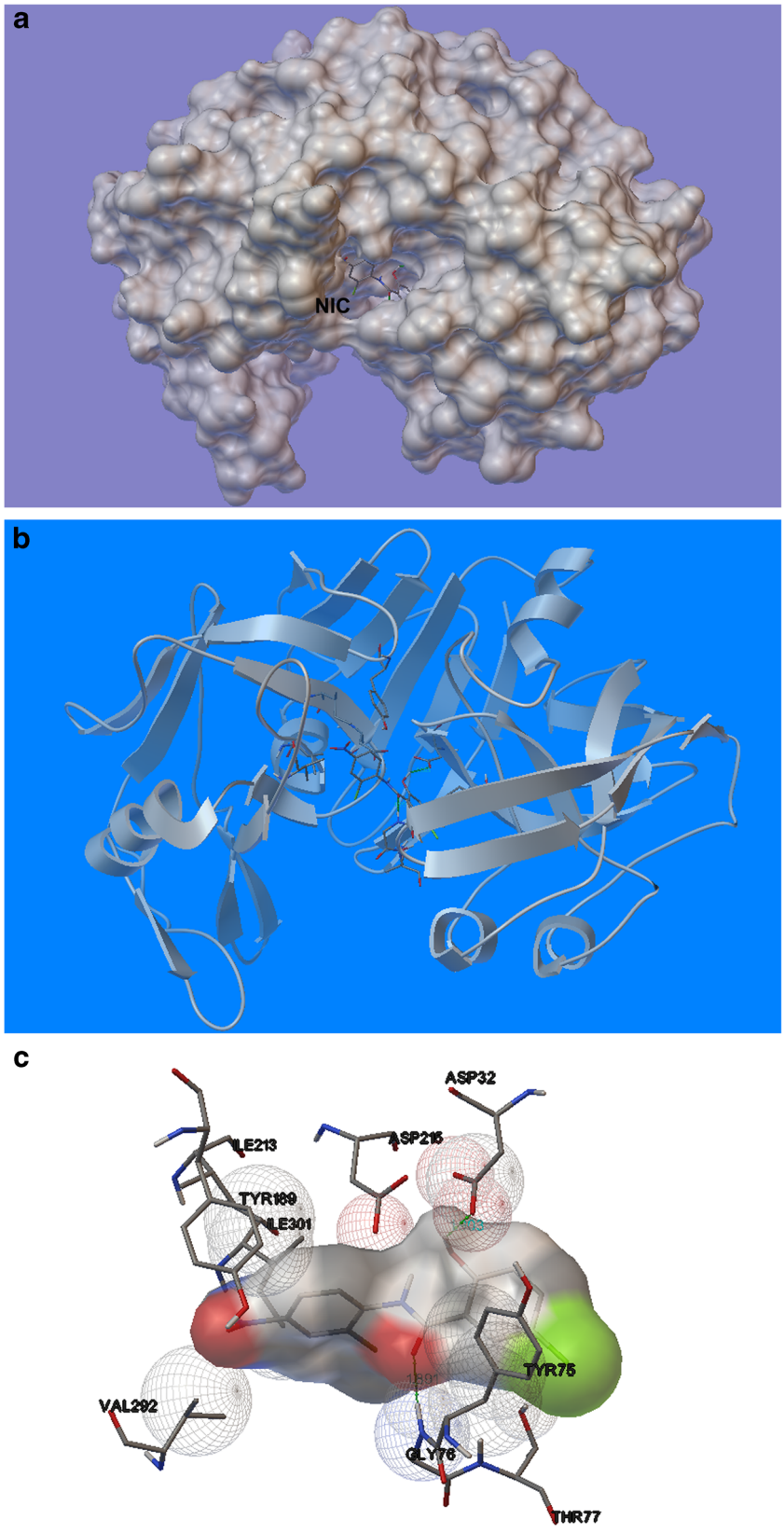

Fig. 12 Binding modes between NIC and pepsin, namely, the hydrophobicity of pepsin with NIC (**a**), the cartoon ribbons of pepsin with NIC (**b**), zoomed-in image of the binding site of pepsin with NIC denoted by sticks (**c**), and molecular modeling of the interaction between NIC and pepsin, with broken lines denoting hydrogen bonds

nonradiative energy transfer and suggests static quenching between NIC and pepsin.

Conformational Investigation

UV–Vis Absorption Spectroscopy

UV–Vis absorption spectra can be utilized to investigate the protein structural changes and protein–ligand complex conformation [43]. The change in absorption spectral of pepsin in the presence of drugs is shown in Fig. 8. The UV–vis spectra of pepsin with intense absorption near 278 nm are attributable to π–π* transitions of the aromatic amino acids Tyr, Trp, and phenylalanine (Phe) [44]. The intensity of the absorption peak at 278 nm increased with the addition of NIC for the ratio of the free drug to NIC–pepsin complex would be increased with increase of the drug concentration, and the absorption maximum exhibited a slight blue-shift toward the lower wavelength region (from 275 to 273 nm). Upon addition of NIC to the solution, the peaks in the far UV region (approximately 250 nm) of the pepsin–NIC complex increased, and the maximum peak position exhibited an evident blue-shift (from 257 to 251 nm) compared with a solution of pepsin at the lowest NIC concentration. The above results implied that as hydrophobicity increased, the peptide strands of pepsin were extended [45], thereby inducing a conformational change in pepsin. NIC binds to pepsin at high affinigy through strong hydrophobic interactions [33].

Synchronous Fluorescence Spectroscopy

Synchronous fluorescence spectroscopy can provide information on the molecular environment in the vicinity of a chromophore. The shift in wavelength of the emission maxima λ_{em} corresponds to the changes of polarity around the chromophore molecule [11]. When the wavelength interval ($\Delta\lambda$) between excitation and emission wavelengths is stabilized at 15 or 60 nm, synchronous fluorescence provides characteristic information on Tyr or Trp residues, respectively [46].

Generally, as the NIC concentration increases, the fluorescence of Trp residues exhibits a blue-shift (from 280 to 278 nm) upon addition of NIC, as shown in Fig. 9. The blue shift of the emission maximum indicates that the hydrophobicity of the Trp residues increased and the Trp buried in the nonpolar hydrophobic cavities were moved to a more hydrophobic environment, resulting in an altered the conformation of pepsin in the presence of NIC [47]. On other hand, the hydrophobic interactions between NIC and Trp residues of pepsin have been enhanced [12]. However, no shift in the maximum emission wavelength occurred at $\Delta\lambda$=15 nm, indicating that NIC has little effect on the microenvironment of Tyr residues in pepsin [48]. The above results indicated that NIC was closer to the Trp residues than to the Tyr residues and the microenvironments of Trp residues were more strongly affected by NIC than the Tyr residues.[37]

Three-Dimensional Fluorescence Spectroscopy

In recent years, three-dimensional fluorescence contour spectra have been extensively used in fluorescence analysis because they can provide additional information or evidence regarding the conformational changes of pepsin in the presence of NIC. Figure 10 shows the three-dimensional fluorescence spectrum of pepsin (a) and NIC–pepsin (b). Peak a represents the Rayleigh scattering peak ($\lambda_{em}=\lambda_{ex}$), and peak 1 ($\lambda_{ex}/\lambda_{em}$=280 nm/336 nm) mainly reveals the spectral features of Tyr and Trp residues. When pepsin is excited at 280 nm, the intrinsic fluorescence of Trp and Tyr residues can be detected, and the fluorescence of Phe residue is negligible [10]. In the presence of NIC, the fluorescence intensity of peak 1 ($\lambda_{em}/\lambda_{ex}$=280/349) decreased from 786.5 to 289.2. The observed large-scale decrease after the addition of NIC implied that changes in the peptide chain structure of pepsin took place. The above results were consistent with of the obtained UV–vis spectra and synchronous fluorescence spectra.

Effect of Salt

To investigate the effects of ionic strength on the binding of NIC to pepsin, a series of fluorescence measurements were obtained with increasing NaCl concentration from 0.1 to 2.0 mol·L^{-1}. The intensity of fluorescence spectra of NIC with pepsin at pH 2.0 decreased slightly as NaCl concentration increased (Fig. 11). This effect can be caused by an increase in the apparent dissociation constant due to the electrostatic screening of salt counterions on both NIC and pepsin [49]. On the other hand, even at a very high ionic strength, the fluorescence attenuation of NIC is still unremarkable, thereby

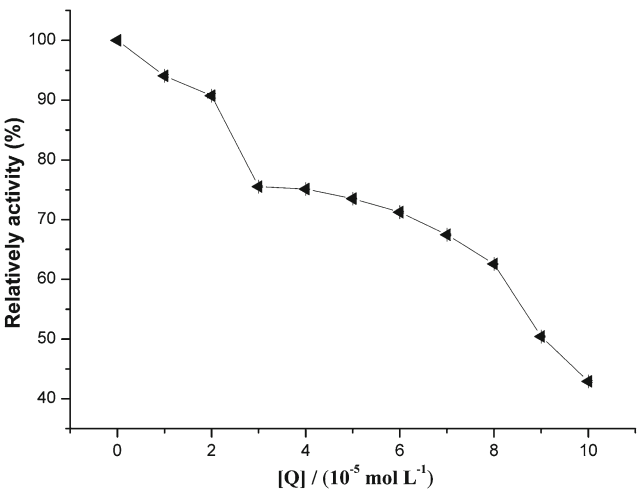

Fig. 13 Pepsin activities in the absence and presence of NIC at different concentrations (pH 2.0, T=310 K), C_{pepsin} =1.0×10^{-5} mol·L^{-1}

suggesting that instead of electrostatic forces, hydrophobic interactions are mainly responsible for the interaction. The observed phenomenon was in accordance with the conclusion deduced from fluorescence data.

Molecular Docking

Molecular docking is a computational technique extensively used in analyzing the interactions between ligands and proteins [50]. The lowest energy ranked results of four NIC–pepsin conformations are listed in Table 3. For all the simulated binding conformations, NIC binds with the pepsin cavity. Moreover, the exact binding sites of NIC on pepsin are different among the six conformations. The exact binding site of NIC on pepsin with the lowest binding free energy is shown in Fig. 12. The docking revealed the most likely binding site in the enzyme. The interaction occurs in the area between domains I and III [11], wherein NIC is surrounded by Asp-32, Asp-215, Thr-77, Tyr-75, Tyr-189, Gly-76, Ile-213, Ile-301, and Val-292. Hydrogen bonds exist between the phenolic hydroxyl of NIC and Asp-32 (with a distance of 1.903 Å) and between the carbonyl group of NIC and Gly-76 (with a distance of 1.891 Å) (Fig. 12c). Moreover, NIC enters the hydrophobic cavity of pepsin via hydrophobic interactions between NIC and pepsin (Fig. 12a and b). The abovementioned results agree well with the aforementioned thermodynamic analysis. Thus, based on docking and synchronous fluorescence results, NIC bound directly to the enzyme cavity site, which subsequently influenced the microenvironment of the catalytic site.

Effect of NIC on Pepsin Activity

The effect of NIC on pepsin activity in vitro was investigated to determine whether NIC can affect the activity of pepsin after entering the organism through food and drugs. The activity of pepsin in the absence of NIC was set to 1, and changes in enzyme activity induced by the presence of different NIC concentrations were measured. As shown in Fig. 13, pepsin activity changed evidently in the presence of NIC. As the NIC concentration increased, the relative pepsin activity significantly decreased. Moreover, 50 % of the relative pepsin activities was approximately 9.01×10^{-5} mol·L^{-1}. The results are consistent with the molecular docking and synchronous fluorescence results and indicated that NIC can inhibit pepsin activity.

Conclusions

Spectrophotometric techniques, such as fluorescence, UV absorption, and synchronous fluorescence spectra, have been successfully applied to investigate the interaction between pepsin and NIC. Fluorescence data showed that the fluorescence quenching mechanism of pepsin occurred mainly through static quenching. Quenching constants (K_b) were obtained using both fluorescence data and UV–vis spectra. Based on the results of thermodynamic parameters and molecular docking study, NIC could spontaneously bind with pepsin mainly through hydrophobic and hydrogen bonds. Results from the salt effect experiment suggest that hydrophobic interactions, not electrostatic interactions, are mainly responsible for the interaction. The distance between NIC and pepsin was sufficiently small (r=2.47 nm) to induce nonradiative energy transfer from pepsin to drug. The synchronous and three-dimensional fluorescence spectra confirmed that binding of NIC to pepsin induced some microenvironmental and conformational changes in pepsin molecules, which could cause inhibition of pepsin activity. The results obtained will be of biological significance for the transportation and distribution of NIC in vivo and beneficial for the investigation of the pharmacological function and dynamics of NIC.

Acknowledgments We gratefully acknowledge the financial support of the Applied Basic Research Project of Sichuan Province (Grant No. 2014JY0042).

References

1. Manek RV, Kolling WM (2004) Influence of moisture on the crystal forms of niclosamide obtained from acetone and ethyl acetate. AAPS PharmSciTech 5(1):1–8. doi:10.1208/pt050114
2. Yo YT, Lin YW, Wang YC, Balch C, Huang RL, Chan MW, Sytwu HK, Chen CK, Chang CC, Nephew KP, Huang T, Yu MH, Lai HC (2012) Growth inhibition of ovarian tumor-initiating cells by niclosamide. Mol Cancer Ther 11(8):1703–1712. doi:10.1158/1535-7163.MCT-12-0002
3. Helfman DM (2011) Niclosamide: an established antihelminthic drug as a potential therapy against S100A4-mediated metastatic colon tumors. JNCI J Natl Cancer Inst 103(13):991–992. doi:10.1093/jnci/djr221
4. Imperi F, Massai F, Ramachandran Pillai C, Longo F, Zennaro E, Rampioni G, Visca P, Leoni L (2013) New life for an old drug: the anthelmintic drug niclosamide inhibits Pseudomonas aeruginosa quorum sensing. Antimicrob Agents Chemother 57(2):996–1005. doi:10.1128/AAC.01952-12
5. Wu CJ, Jan JT, Chen CM, Hsieh HP, Hwang DR, Liu HW, Liu CY, Huang HW, Chen SC, Hong CF, Lin RK, Chao YS, Hsu JT (2004) Inhibition of severe acute respiratory syndrome coronavirus replication by niclosamide. Antimicrob Agents Chemother 48(7):2693–2696. doi:10.1128/AAC.48.7.2693-2696.2004
6. Gritti I, Banfi G, Roi GS (2000) Pepsinogens: physiology, pharmacology pathophysiology and exercise. Pharmacol Res: Off J Ital Pharmacol Soc 41(3):265–281. doi:10.1006/phrs.1999.0586
7. Ying M, Huang F, Ye H, Xu H, Shen L, Huan T, Huang S, Xie J, Tian S, Hu Z, He Z, Lu J, Zhou K (2015) Study on interaction between curcumin and pepsin by spectroscopic and docking methods. Int J Biol Macromol 79:201–208. doi:10.1016/j.ijbiomac.2015.04.057
8. Spelzini D, Peleteiro J, Pico G, Farruggia B (2008) Polyethyleneglycol-pepsin interaction and its relationship with protein partitioning in aqueous two-phase systems. Colloids Surf B: Biointerfaces 67(2):151–156. doi:10.1016/j.colsurfb.2008.06.013

9. Andreas Scorilas EPD, Levesque MA et al (1999) Immunoenzymatically determined pepsinogen C concentration in breast tumor cytosols: an independent favorable prognostic factor in node-positive patients. Clin Cancer Res 5:1778–1785
10. Zeng HJ, You J, Liang HL, Qi T, Yang R, Qu LB (2014) Investigation on the binding interaction between silybin and pepsin by spectral and molecular docking. Int J Biol Macromol 67:105–111. doi:10.1016/j.ijbiomac.2014.02.051
11. Zhang H, Cao J, Fei Z, Wang Y (2012) Investigation on the interaction behavior between bisphenol A and pepsin by spectral and docking studies. J Mol Struct 1021:34–39. doi:10.1016/j.molstruc.2012.04.072
12. Li Z, Li Z, Yang L, Xie Y, Shi J, Wang R, Chang J (2015) Investigation of the binding between pepsin and nucleoside analogs by spectroscopy and molecular simulation. J Fluoresc 25(2):451–463. doi:10.1007/s10895-015-1532-2
13. Lian S, Wang G, Zhou L, Yang D (2013) Fluorescence spectroscopic analysis on interaction of fleroxacin with pepsin. Lumin: J Biol Chem Lumin 28(6):967–972. doi:10.1002/bio.2469
14. Fan Y, Zhang S, Wang Q, Li J, Fan H, Shan D (2013) Investigation of the interaction of pepsin with ionic liquids by using fluorescence spectroscopy. Appl Spectrosc 67(6):648–655. doi:10.1366/12-06793
15. Cha KH, Cho KJ, Kim MS, Kim JS, Park HJ, Park J, Cho W, Park JS, Hwang SJ (2012) Enhancement of the dissolution rate and bioavailability of fenofibrate by a melt-adsorption method using supercritical carbon dioxide. Int J Nanomedicine 7:5565–5575. doi:10.2147/IJN.S36939
16. Maltas E (2014) Binding interactions of niclosamide with serum proteins. J Food Drug Anal 22(4):549–555. doi:10.1016/j.jfda.2014.03.004
17. Anson ML (1938) The estimation of pepsin, trypsin, papain, and cathepsin with hemoglobin. J Gen Physiol 22(1):79–89
18. Padmanabhan J, Parthasarathi R, Subramanian V, Chattaraj PK (2006) Group philicity and electrophilicity as possible descriptors for modeling ecotoxicity applied to chlorophenols. Chem Res Toxicol 19(3):356–364. doi:10.1021/tx050322m
19. Parr RG, Yang W (1989) Density functional theory of atoms and molecules. Oxford University Press, Oxford
20. Raymond P, Iczkowski JLM (1961) Electronegativity. J Am Chem Soc 83(17):3547–3551
21. Pearson RG (1997) Chemical hardnesss. Applications from molecules to solids. VCH-Wiley, Weinheim
22. Teng Y, Liu R, Li C, Xia Q, Zhang P (2011) The interaction between 4-aminoantipyrine and bovine serum albumin: multiple spectroscopic and molecular docking investigations. J Hazard Mater 190(1–3):574–581. doi:10.1016/j.jhazmat.2011.03.084
23. Hu Y-J, Liu Y, Zhang L-X, Zhao R-M, Qu S-S (2005) Studies of interaction between colchicine and bovine serum albumin by fluorescence quenching method. J Mol Struct 750(1–3):174–178. doi:10.1016/j.molstruc.2005.04.032
24. Dong C, Ma S, Liu Y (2013) Studies of the interaction between demeclocycline and human serum albumin by multi-spectroscopic and molecular docking methods. Spectrochim Acta A Mol Biomol Spectrosc 103:179–186. doi:10.1016/j.saa.2012.10.050
25. Hu Y-J, Liu Y, Shen X-S, Fang X-Y, Qu S-S (2005) Studies on the interaction between 1-hexylcarbamoyl-5-fluorouracil and bovine serum albumin. J Mol Struct 738(1–3):143–147. doi:10.1016/j.molstruc.2004.11.062
26. Tajmir-Riahi HA, Mandeville JS (2010) Complexes of dendrimers with bovine serum albumin. Biomacromolecules 11:465–472
27. Bi S, Ding L, Tian Y, Song D, Zhou X, Liu X, Zhang H (2004) Investigation of the interaction between flavonoids and human serum albumin. J Mol Struct 703(1–3):37–45. doi:10.1016/j.molstruc.2004.05.026
28. Zhang YZ, Zhou B, Zhang XP, Huang P, Li CH, Liu Y (2009) Interaction of malachite green with bovine serum albumin: determination of the binding mechanism and binding site by spectroscopic methods. J Hazard Mater 163(2–3):1345–1352. doi:10.1016/j.jhazmat.2008.07.132
29. Susana Soares NM, de Freitas V (2007) Interaction of different polyphenols with Bovine Serum Albumin (BSA) and Human Salivary r-Amylase (HSA) by fluorescence quenching. J Agric Food Chem 55(16):6726–6735. doi:10.1021/jf070905x
30. Lakowica JR GW, 12 (1973) 4161. Quenching of fluorescence by oxygen. Probe for structural fluctuations in macromolecules. Biochemistry 12 (21):4161–4170
31. Ware WR (1962) Oxygen quenching of fluorescence in solution: an experimental study of the diffusion process. J Phys Chem 66(3):455–458. doi:10.1021/j100809a020
32. Shilpa Dogra PA, Nair M, Barthwal R (2013) Interaction of anticancer drug mitoxantrone with DNA hexamer sequence d-(CTCGAG)2 by absorption, fluorescence and circular dichroism spectroscopy. J Photochem Photobiol B Biol 123:48–54. doi:10.1016/j.jphotobiol.2013.03.015
33. He LL, Wang X, Liu B, Wang J, Sun YG, Gao EJ, Xu SK (2011) Study on the interaction between promethazine hydrochloride and bovine serum albumin by fluorescence spectroscopy. J Lumin 131(2):285–290. doi:10.1016/j.jlumin.2010.10.014
34. Ross PD, Subramanian S (1981) Thermodynamics of protein association reactions: forces contributing to stabilit. Biochemistry 20(11):3097–3102. doi:10.1021/bi00514a017
35. Becktel WJSJ (1987) Protein stability curves. Biopolymers 26(11):1859–1877. doi:10.1002/bip.360261104
36. Shen LL, Xu H, Huang FW, Li Y, Xiao HF, Yang Z, Hu ZL, He ZD, Zeng ZL, Li YN (2015) Investigation on interaction between Ligupurpuroside A and pepsin by spectroscopic and docking methods. Spectrochim Acta A 135:256–263. doi:10.1016/j.saa.2014.06.087
37. Zeng HJ, Qi TT, Yang R, You J, Qu LB (2014) Spectroscopy and molecular docking study on the interaction behavior between nobiletin and pepsin. J Fluoresc 24(4):1031–1040. doi:10.1007/s10895-014-1379-y
38. Zeng HJ, Liang HL, You J, Qu LB (2014) Study on the binding of chlorogenic acid to pepsin by spectral and molecular docking. Lumin: J Biol Chem Lumin 29(7):715–721. doi:10.1002/bio.2610
39. Gao XY, Zhang XJ, Tang YC, Zhang XP, Zhao WJ, Zi YQ (2011) Analysis of binding interaction between prulifloxacin and pepsin in the existence of Eu(III): A spectroscopic analysis. Curr Anal Chem 7(3):194–200
40. Förster T (1965) Delocalized excitation and excitation transfer, vol 3, Modern Quantum Chemistry. Academic, New York
41. Horrocks WD, Collier WE (1981) Lanthanide ion luminescence probes. Measurement of distance between intrinsic protein fluorophores and bound metal ions: quantitation of energy transfer between tryptophan and terbium(III) or europium(III) in the calcium-binding protein parvalbumin. J Am Chem Soc 103(10):2865–2862
42. Jin J, Zhang X (2008) Spectrophotometric studies on the interaction between pazufloxacin mesilate and human serum albumin or lysozyme. J Lumin 128(1):81–86. doi:10.1016/j.jlumin.2007.05.008
43. Teng Y, Zhang H, Liu R (2011) Molecular interaction between 4-aminoantipyrine and catalase reveals a potentially toxic mechanism of the drug. Mol BioSyst 7(11):3157–3163. doi:10.1039/c1mb05271c
44. Qian ZM, Li H, Sun H, Ho K (2002) Targeted drug delivery via the transferrin receptor-mediated endocytosis pathway. Pharmacol Rev 54(4):561–587. doi:10.1124/pr.54.4.561
45. Donovan JW (1969) Changes in ultraviolet absorption produced by alteration of protein conformation. J Biol Chem 244(8):1961–1967

46. Guo M, Lu WJ, Li MH, Wang W (2008) Study on the binding interaction between carnitine optical isomer and bovine serum albumin. Eur J Med Chem 43(10):2140–2148. doi:10.1016/j.ejmech.2007.11.006
47. Changwei Liu AB, Cheng G, Lin X, Dong S (1998) Characterization of the structural and functional changes of hemoglobin in dimethyl sulfoxide by spectroscopic techniques. Biochim Biophys Acta 1385:53–60
48. Wang Q, Yan J, He J, Bai K, Li H (2013) Characterization of the interaction between 3-oxotabersonine and two serum albumins by using spectroscopic techniques. J Lumin 138:1–7. doi:10.1016/j.jlumin.2013.01.035
49. Favilla R, Mazzini A, Cavatorta P, Sorbi RT, Sartor G (1993) The Interaction of 4′, 6-Diamidino-2-phenylindole (DAPI) with Pepsin. J Fluoresc 3(4):229–232
50. He J, Wang Q, Zhang L, Lin X, Li H (2014) Docking simulations and spectroscopy of the interactions of ellagic acid and oleuropein with human serum albumin. J Lumin 154:578–583. doi:10.1016/j.jlumin.2014.06.002